Infrared Photodissociation Spectroscopy of the Benzoic Acid Radical Cation in a Quadrupole Trap

Jos Oomens,*,† Gert von Helden,‡ and Gerard Meijer‡

FOM Institute for Plasma Physics "Rijnhuizen", Edisonbaan 14, 3439MN Nieuwegein, The Netherlands, and Fritz-Haber-Institut der Max-Planck-Gesellschaft Faradayweg 4-6, 14195 Berlin, Germany

The vibrational spectrum of the gas-phase benzoic acid radical cation is reported in the fingerprint region from 500 to 1800 cm^{-1}. The benzoic acid cation is produced either via $(1 + 1')$ resonance-enhanced multiphoton ionization or via chemical ionization of benzoic acid vapor. The ions are stored and mass-selectively isolated in a quadrupole ion trap where they are irradiated with the output of a widely tunable infrared free electron laser. Upon resonance, photodissociation occurs and recording the total fragment-ion yield as a function of wavelength yields the infrared spectrum. The experimental spectrum suggests that the ion is effectively planar, although a density functional theory calculation predicts a staggered structure to be the lowest in energy. In addition, we tentatively identify the infrared spectrum of protonated benzoic acid.

1. Introduction

The infrared spectroscopy of gas-phase molecular ions has long been impeded by the low densities in which these species can be produced.[1] Small molecular ions can be produced relatively efficiently in electron impact and discharge sources so that sensitive direct absorption techniques, e.g., laser absorption combined with phase-sensitive detection, can be applied.[2−5] However, fragmentation becomes a serious problem for larger molecular ions, which therefore require more gentle ionization techniques and/or mass selective detection. A drawback of these techniques lies in the fact that ion densities are even further reduced so that direct absorption methods become difficult if not impossible. Several inventive detection schemes have been developed over the past two decades to replace conventional infrared techniques.[1]

Threshold ionization techniques, most notably zero-electron kinetic energy (ZEKE[6]) spectroscopy and mass analyzed threshold ionization (MATI[7]) spectroscopy, have been widely applied to obtain information on the vibrational structure of the ionic ground state. However, no direct IR spectral information on the ground electronic state of the cation is obtained with these techniques, as transitions between (rovibrational levels in) electronic states of the neutral molecules are induced and hence different selection rules apply. Another commonly used technique, the "messenger" technique,[8] employs tagging of a jet-cooled molecular ion with a weakly bound messenger atom (or small molecule). This complex dissociates upon infrared absorption, which can be monitored in a time-of-flight (TOF) mass spectrometer. The method relies on the weak interaction between the messenger atom and the ionic chromophore, and the observed IR absorption spectrum of the complex is expected to closely resemble that of the bare ion. It has also been shown that the infrared spectrum of a neutral molecule in a long-lived high Rydberg state, where the outermost electron is far away from the ionic core, resembles that of the corresponding

molecular ion very closely.[9] Thus, infrared-induced ionization of Rydberg neutrals and subsequent ion detection in a TOF mass spectrometer can be used to obtain their IR spectra, although the auto-ionization rate, and hence the intensities in the IR spectrum, may show vibrational mode dependency as it relies on (coincidental and unknown) vibronic couplings.

By use of a powerful infrared laser source, it is possible to dissociate molecular ions stored in an ion trap in a multiple photon-absorption process.[10,11] This was first shown to be possible using CO_2 lasers,[12,13] which possess only limited and discontinuous tunability, however. Recently, we have shown that a widely tunable free-electron laser can also be used as infrared source,[14] and later, it was shown that this method is also applicable in various more sophisticated ion-trapping devices.[15−17] Fingerprint infrared spectra have been reported for a variety of cationic polyaromatic hydrocarbons (PAHs),[14,18,19] which were generated by nonresonant UV ionization using the focused output of an ArF excimer laser. For more fragile species, such as many biochemically relevant species, this ionization scheme may cause substantial, or even complete, fragmentation. We know from our earlier studies that UV irradiation of benzoic acid at 193 nm causes complete photofragmentation as well.[20] Alternatively, external ion production and injection into an ion trap for IR multiple photon dissociation (IRMPD) spectroscopy has been used for a variety of cluster ions.[15,21] In the current study, we present the infrared spectrum of the benzoic acid cation, generated in situ in the ion trap via two different gentle ionization methods. It is shown that two-color resonance-enhanced multiphoton ionization (REMPI) as well as chemical ionization (CI) can produce the intact benzoic acid ion in our trap for subsequent IRMPD spectroscopy.

Neutral benzoic acid has been intensively studied spectroscopically as it is considered a benchmark biochemical compound,[22] particularly in view of its strong ability to form dimers through a double hydrogen bond.[23,24] However, to our knowledge, no infrared spectral information on the cation has been reported to date. It is important to note that the lifetime of the S_1 electronic state of the benzoic acid monomer is extremely short[25] due to intersystem crossing, which causes sub-picosecond

* To whom correspondence may be addressed. E-mail: joso@rijnh.nl.
† FOM Institute for Plasma Physics "Rijnhuizen".
‡ Fritz-Haber-Institut der Max-Planck-Gesellschaft.

relaxation into the triplet state. Since both the messenger technique as well as threshold ionization techniques commonly utilize a well-defined electronically excited intermediate state, the short S_1 lifetime severely limits or even prevents recording of the IR spectrum of the benzoic acid cation via either one of these methods.

In addition to the benzoic acid cation, we have identified the infrared spectrum of protonated benzoic acid in the CI experiments. Infrared spectroscopy of protonated species, which are of obvious interest in a wide range of biochemical processes, dates back to the late 70s and early 80s, when studies on several small systems such as H_3O^+,[2] H_3^+,[3] and HCO^+,[4] were reported. In recent years, infrared spectroscopy has been successfully applied to investigate larger protonated species in the gas phase, aiming particularly at the determination of the protonation sites.[26-29] In the case of benzoic acid presented here, comparison of the experimental spectrum to the results of a density functional theory (DFT) calculation, clearly indicates that protonation occurs at the carbonyl oxygen atom.

2. Experimental Section

The experimental apparatus, as it has been used to study cationic PAHs, is described in detail elsewhere.[14] Briefly, vapor-phase molecules are ionized using different methods (see below) and are stored in a quadrupole ion trap.[30-32] The parent ion can be isolated by axial ejection of UV-induced fragments from the ion trap using a 2-ms increase in the rf amplitude.[32] The isolated parent ions are subsequently irradiated with one or more pulses of the Free Electron Laser for Infrared eXperiments (FELIX). FELIX delivers 5 μs long widely tunable (5−250 μm) high energy (∼60 mJ) laser pulses at a 5-Hz repetition rate.[33] The laser beam is focused to a sub-millimeter spot in the center of the ion trap. When the infrared wavelength is in resonance with an absorption band of the ion, incoherent multiple photon absorption mediated by intramolecular vibrational redistribution (IVR) can take place.[10,11] Because of the high intensity of FELIX, internal energies may reach levels beyond the dissociation threshold so that the ion can undergo fragmentation. For the benzoic acid cation, the dissociation energy is calculated to be only 1.9 eV.[20] After the infrared interaction, the ions are pulse extracted from the trap and are analyzed in a 60 cm long TOF mass spectrometer, equipped with a multichannel plate (MCP) detector.[34] The MCP transient is recorded and averaged using a digital oscilloscope. To obtain the infrared spectrum, the fragment yield is recorded as a function of FELIX wavelength. Despite the complicated dependence of the IRMPD efficiency on laser power,[35] the spectra have been linearly corrected for variations in the FELIX pulse energy, which was measured immediately after each wavelength scan. The approximation of a linear power dependence was previously found to be adequate,[14] although particularly for species with very high dissociation thresholds, higher order dependencies (up to quadratic) have been found.[19]

Unlike PAHs, which have been efficiently ionized through nonresonant two-photon UV excitation with a 193-nm (6.4-eV) excimer laser,[14,18,19] benzoic acid completely fragments upon exposure to the focused ArF ionization laser, forming mainly the benzoyl cation $C_6H_5CO^+$ at $m/z = 105$.[20] Using an unfocused ArF laser or using KrF (248 nm/5.0 eV) instead of ArF does not remedy this problem. Calculated ion energetics of benzoic acid[20] predict that, upon excimer laser irradiation, the benzoyl radical will be formed via one-photon absorption, since the dissociation threshold of 4.7 eV is much lower than the ionization potential (IP) of 9.1 eV. The benzoyl radical can then
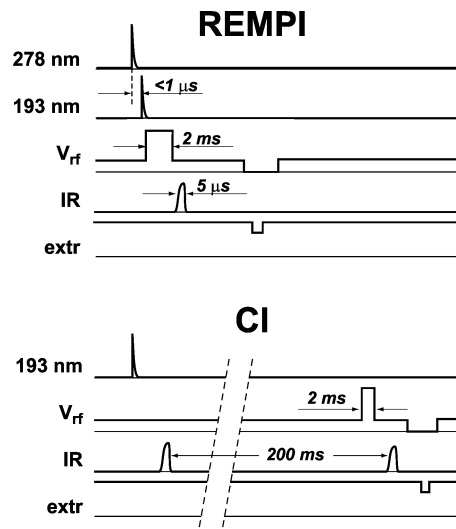
Figure 1. Timing sequences for the two experiments using REMPI and chemical ionization. The traces indicate the dye laser pulse (278 nm), the ArF laser pulse (193 nm), the rf amplitude (V_{rf}), the FELIX pulse (IR), and the ion extraction pulse (extr). Some typical time scales are indicated.

photoionize by absorption of a second UV photon (IP = 6.3 eV). These ion energetics, which prevent the direct formation of benzoic acid ions, can be summarized as follows (all values in eV)
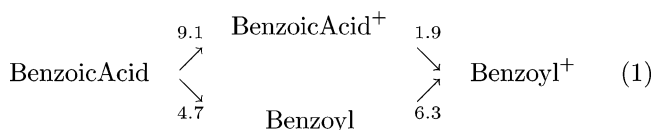
Therefore, two different approaches are used in this study to produce the intact benzoic acid cation in our ion trap for subsequent recording of its infrared spectrum via IRMPD spectroscopy.

First, we applied a two-color REMPI scheme, using the unfocused frequency doubled output of a pulsed dye laser at 556 nm (generated using a mixture of Rhodamine 6G and Rhodamine 575 dyes) to resonantly excite to the S_1 state.[25] The (unfocused) ArF laser then one-photon ionizes the molecule from the triplet state. The long lifetime of the triplet state makes that the timing between the two lasers is relatively uncritical, and in practice, the delay is kept ≤1 μs. The complete timing sequence for the experiment, showing the two UV lasers, the rf amplitude, the infrared laser pulse, and the ion extraction pulse, is sketched in the upper panel of Figure 1. Although this ionization method still also induced substantial fragmentation (see upper trace in Figure 2), these UV induced fragments are easily removed from the trap using a 2 ms long increase of the rf amplitude (see Figure 1). This causes a temporary shift of the low-mass cutoff of the ion trap to higher m/z values, which axially ejects all ions with a mass lower than that of the benzoic acid cation (middle trace in Figure 2). The lower trace shows the mass spectrum after IRMPD at $\lambda = 9$ μm of the isolated benzoic acid cation resulting mainly in the appearance of the benzoyl cation as fragment. Note that the peak at $m/z = 137$ is due to contamination of the vacuum chamber with PABA (para-amino benzoic acid, $H_2N-C_6H_4-COOH$), which is known to fragment into mass channels 120, 92, and 65,[36] and its presence should therefore have no influence on the spectra observed in this study.

Second, it is possible to form intact benzoic acid cations via chemical ionization, i.e., via charge transfer from trapped ionic

IR Spectrum of the Benzoic Acid Radical Cation

J. Phys. Chem. A, Vol. 108, No. 40, 2004 **8275**
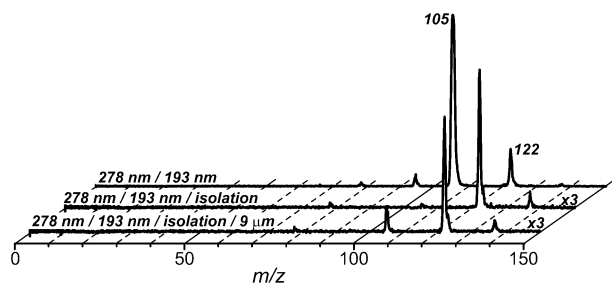
Figure 2. Mass spectra of the benzoic acid cation recorded at various stages in the experimental cycle. The upper trace shows the benzoic acid ion ($m/z = 122$) and fragment ions produced by the two-color REMPI method. The second trace shows the effect of rf axial ejection of fragment ions isolating the parent ion and higher mass ions. The lower trace results from IRMPD of the benzoic acid cation with FELIX. Note that the lower two traces are multiplied by a factor of 3.
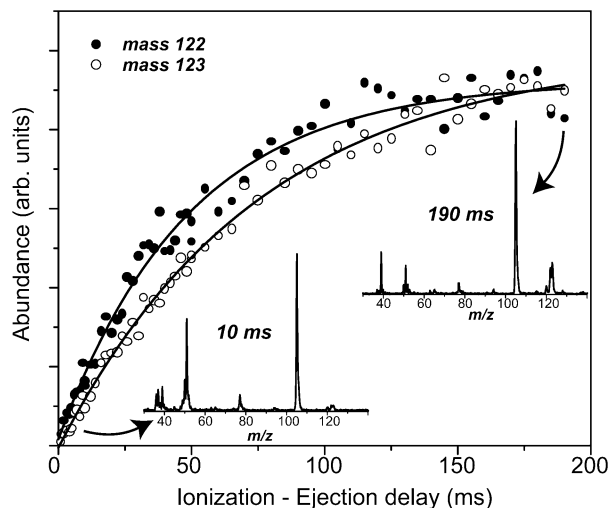
Figure 3. Abundance of the benzoic acid cation (●) and its protonated counterpart (○) as a function of the time delay between the UV pulse from the ArF laser and extraction from the trap into the TOF mass spectrometer. The lines represent fits to a function of the form $1 - \exp(-kt)$. Actual mass spectra taken with 10 ms and 190 ms reaction delay are shown in the insets; masses 122 and 123 are seen to increase at the expense of the abundance of lighter ions. Note that the ArF laser ionization scheme induces substantially more fragmentation than the two-color REMPI scheme (Figure 2).

fragments to neutral benzoic acid. This is shown in Figure 3, where the time delay between UV laser ionization and the rf ejection pulse is scanned, while extraction from the trap into the TOF mass spectrometer is fixed at 200 ms (no IRMPD is applied). At $\Delta t = 0$, there are no benzoic acid ions due to complete fragmentation[20] and the charge-transfer reaction follows a $1 - \exp(-kt)$ behavior. In addition, we observe that in this process not only the benzoic acid cation at $m/z = 122$ is produced but also the protonated species at $m/z = 123$. The insets in Figure 3 show two mass spectra taken at short and long reaction delays, clearly showing how benzoic acid cations are formed at the expense of smaller fragment ions. Note that charge transfer to benzoic acid does not occur from the benzoyl cation, which is indeed not expected based on their respective IPs (see eq 1). These processes can be summarized as

$$\text{charge transfer } M^+ + C_7H_6O_2 \rightarrow M + C_7H_6O_2{}^+ \quad (2)$$

$$\text{proton transfer } MH^+ + C_7H_6O_2 \rightarrow M + C_7H_7O_2{}^+ \quad (3)$$
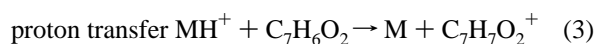
where the IP of M should be higher than 9.1 eV for reaction 2
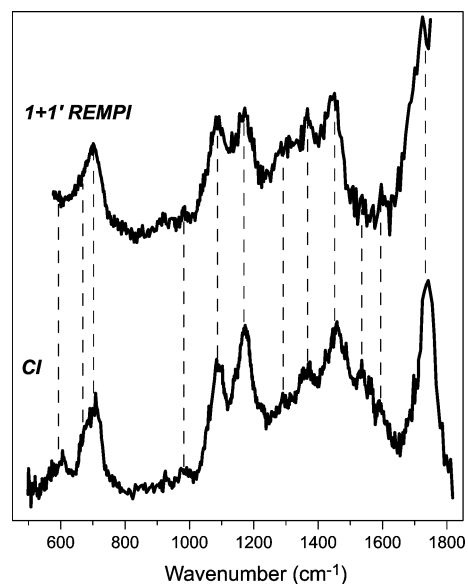
Figure 4. Experimental IRMPD spectra of the benzoic acid cation for ions produced via two-color REMPI and for ions produced via chemical ionization. The vertical dashed lines refer to bands listed in Table 1.

to occur and the proton affinity (PA) of M should be lower than 8.5 eV, being the PA of benzoic acid,[37] for reaction 3 to occur.

To record the infrared spectrum, the extraction delay is set to 207 ms and the ejection pulse, ejecting all species with $m/z \leq 120$, is applied 190 ms after the UV pulse, as sketched in the lower panel of Figure 1. Thus, the first FEL pulse is "wasted", and only the second pulse is used to measure the infrared spectrum via IRMPD.

3. Results and Discussion

The infrared spectrum obtained via IRMPD represents a multiple-photon absorption spectrum, which in general deviates somewhat from a linear absorption spectrum. Because of anharmonic interactions in the vibrationally highly excited species, the infrared bands generally show a red shift as well as substantial broadening. In the wavelength range studied here, red shifts for various covalently bound systems were found to be typically 5−30 cm^{-1}, whereas line widths are on the order of 30 cm^{-1}.[14] Furthermore, the red shift is dependent on the dissociation threshold as was explicitly shown for the para-amino benzoyl ion.[36]

Upon resonant infrared irradiation, the benzoic acid cation fragments mainly into the benzoyl cation with a mass of $m/z = 105$. Weak fragmentation signals are observed in the phenyl mass channel at $m/z = 77$ as well. Infrared-induced dissociation is also observed at $m/z = 79$ in the CI experiments, which is likely due to fragmentation of protonated benzoic acid (see below). To obtain the infrared spectrum of the benzoic acid cation, the intensity in both fragment channels is summed and divided by the total ion signal, while the wavelength of the FEL is scanned.

The IRMPD spectrum of the benzoic acid cation, recorded using the two different parent ion preparation methods, is shown in Figure 4. The two spectra are very similar, both in terms of line positions and relative intensities, and even weak features such as those at 979 and 1595 cm^{-1} appear to reproduce correctly. Small discrepancies are observed in the 1500−1600 cm^{-1} range, and a possible explanation for this is given below. Despite the fairly broad and sometimes congested spectral

8276 *J. Phys. Chem. A, Vol. 108, No. 40, 2004*

Oomens et al.

TABLE 1: Infrared Spectrum of the Benzoic Acid Cation

mode[b]	DFT calculated[a] (C_s)		observed	
	ν	I_{rel}[c]	ν	I_{rel}
β'_{OH}	622	0.24	604	0.06
$\beta'_{CH}\beta'_{OH}$	691	0.71	677	0.17
$\alpha_{OCO}\beta_{OH}$	711	0.24	709	0.36
β_{CH}	976	0.22	979	0.05
β_{CH}	1080	0.29	1090	0.60
β_{OH}	1199	0.89	1173	0.79
			≈1290	
β_{CH}, β_{OH}	1361	0.34	1362	0.57
$\beta_{CH}, \beta_{OH}\sigma_{CC}$	1425	0.51	1456	0.79
β_{CH}, β_{OH}	1440	0.24		
$\beta_{CH}\sigma_{CC}$	1535	0.21	1534	≈0.30
σ_{CC}	1630	0.14	1593	≈0.20
σ_{CO}	1743	1.00	1738	1.00

[a] B3LYP/D95(d,p). One imaginary frequency (see text). [b] α = scissor; β' = out-of-plane bend; β = in-plane bend; σ = stretch. [c] Only bands with $I_{rel} > 0.10$ are listed.
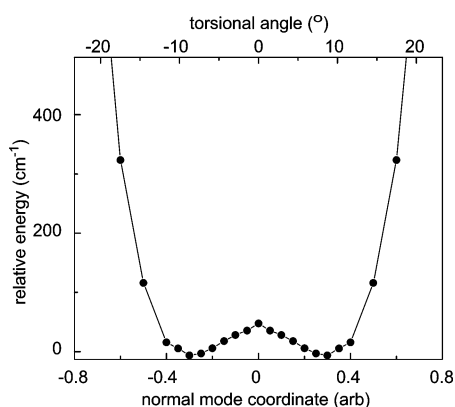
Figure 5. Single-point calculations along the "torsional" normal mode coordinate of the planar (C_s) benzoic acid cation reveal a double-well potential. The energies have been corrected for the zero-point energy (excluding the torsional mode). The corresponding angle between the aromatic and COOH planes is indicated.

features, band positions can still be distinguished reasonably well and they are listed together with their relative intensities in Table 1. The experimental spectrum is compared to results from DFT calculations using the B3LYP functional and the D95(d,p) basis set.[38]

Assuming a planar C_s geometry for the ion, the calculation generates one imaginary frequency ($105i$ cm^{-1}), indicating that the calculated equilibrium structure is actually a saddle point on the potential-energy surface. The imaginary frequency, which is consistently found using different basis sets (3-21G, 4-31G, D95(d,p), 6-31G**) as well as applying the MP2 level of theory, is associated with the torsional motion of the COOH group relative to the benzenoid plane. Scanning the potential-energy surface along the corresponding normal coordinate indeed reveals a double well potential as shown in Figure 5, with the planar configuration being at the local maximum. Reoptimization (B3LYP/D95(d,p)) of the nonplanar structure with C_1 symmetry lowers the energy by about 395 cm^{-1} relative to the planar C_s geometry. In this optimized structure, the angle between the COOH plane and the aromatic plane becomes about 35°.

Both the C_s and the C_1 calculated spectra are compared to the experimental spectrum in Figure 6. Although the torsional mode is located far outside the spectral region studied here, the two theoretical spectra are substantially different in this range as well. The match with the planar C_s geometry is clearly better than with the staggered geometry, which is particularly evident
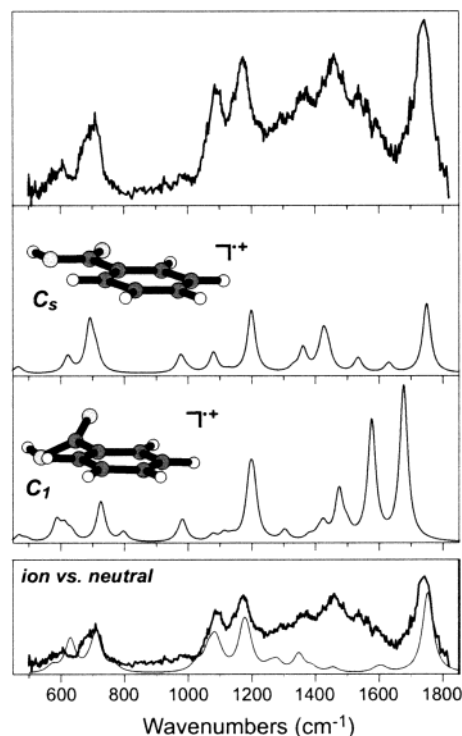
Figure 6. Experimental IRMPD spectrum of the benzoic acid cation (upper panel) compared to results from DFT calculations (unscaled) assuming a planar C_s geometry and a staggered C_1 geometry. The C_1 geometry has the lowest energy, however, the match with experiment appears better for the C_s geometry. The lower panel shows a comparison of the cation spectrum (thick) to that of neutral benzoic acid (thin, data taken from ref 24).

in the 1500−1800-cm^{-1} range. In this range, only one strong band, the CO stretch vibration, is found in agreement with the planar geometry calculation, whereas the C_1 calculation predicts two strong bands. Moreover, the C_s calculation yields a better agreement in line position for this band. In addition, the C_s calculation reproduces the double peak structure around 1100 cm^{-1} and the CH out-of-plane modes around 700 cm^{-1}, substantially better than the C_1 calculation. Therefore, in Table 1, the experimental spectrum is compared to the C_s calculation, which shows fairly good agreement. The main absorption bands can be well recognized and assigned, although, particularly in the congested spectral region between 1250 and 1600 cm^{-1}, assignments are somewhat speculative. The shape of the feature observed around 700 cm^{-1} suggests that it consists of at least two bands, in agreement with calculated bands at 691 and 711 cm^{-1}. Relative intensities show some discrepancies, particularly for the band calculated at 976 cm^{-1} and moreover in the congested region between 1250 and 1600 cm^{-1}, where in general more intensity is observed than calculated. Note that the general red shift of the experimental spectrum with respect to theory is due to a combination of the effects of anharmonicity in the multiple photon absorption process[35] and the typical overestimation of vibrational frequencies of 2−3% by the B3LYP functional used in conjunction with a basis set containing polarization functions.[40]

As mentioned, the barrier to planarity is calculated to be around 400 cm^{-1}. However, from a direct count of vibrational states (based on the calculated harmonic frequencies), the internal energy of the benzoic acid cation at room temperature is estimated to be around 1070 cm^{-1}. In addition, the zero-point-energy difference between the minimum nonplanar structure and the planar "transition-state" geometry is calculated to

IR Spectrum of the Benzoic Acid Radical Cation

J. Phys. Chem. A, Vol. 108, No. 40, 2004 **8277**

be about 160 cm^{-1}. As seen in Figure 5, the torsional potential exhibits two equivalent minima and therefore, at energies high above the barrier the ion is essentially planar.

At this point, it is interesting to briefly speculate on the discrepancies between the REMPI and CI spectra in the 1500–1600-cm^{-1} range (see Figure 4), as they could be related to differences in the internal energy of the ions created via the two ionization methods. The REMPI scheme involves a singlet–triplet intersystem crossing after the excitation step, which deposits energy in the vibrational levels of the triplet state. Although the S–T energy difference is not accurately known, it may be estimated to be on the order of 1 eV.[25] On the basis of Franck–Condon overlap arguments, it may also be assumed that this vibrational excitation is retained in the ionic state. On the other hand, the ions created via CI are approximately at room temperature and hence possess a much lower internal energy than the REMPI ions. In fact, assuming a Boltzmann vibrational state distribution, we calculate that, at room temperature, 18% of the molecules has an internal energy lower than 400 cm^{-1}, i.e. lower than the barrier to planarity. At an average internal energy of around 1 eV, this fraction is practically zero (~0.01%). One could then argue that in the CI ion spectrum, some remnants of the nonplanar minimum energy structure are still observable, particularly between 1500 and 1600 cm^{-1}, where a strong band is predicted for the C_1 structure. However, a second explanation is conceivable: protonated benzoic acid, which is formed by CI but not by REMPI, could dissociate (partly) into the 105 mass channel. As shown below, protonated benzoic acid possesses strong absorption bands in the 1500–1600-cm^{-1} range. If this latter explanation is the correct one, the amount of "cross-talk" can be estimated from the observed intensity between 1500 and 1600 cm^{-1} relative to the intensity of the CO stretch mode at 1743 cm^{-1}. The intensities of the corresponding bands in the calculated spectra of the benzoic acid cation (235 km/mol) and protonated benzoic acid (1160 km/mol, sum of 4 bands) then indicate that the contribution of protonated benzoic acid to the spectrum of cationic benzoic acid is less than 5%.

In the lower panel of Figure 6, we compare our spectrum with the jet-cooled linear-IR absorption spectrum of neutral benzoic acid,[24,39] which is known to be planar. Note the enhanced intensities in the CC stretching and in-plane CH bending range around 1200–1600 cm^{-1} in the spectrum of the cation relative to that in the spectrum of the neutral species. This is similar to what is observed for ionic PAHs, where a π-electron is removed.[40,41]

In the CI experiment, proton transfer to benzoic acid occurs in addition to charge transfer. As seen in Figure 3, the two processes have similar rate constants, resulting in an almost 50/50 mixture of cationic and protonated benzoic acid. On account of the multiplexing nature of the TOF mass spectrometer and the fact that the protonated benzoic acid is not ejected during the isolation step, its infrared spectrum is likely hidden in the data. However, it is not a priori clear what the IRMPD product mass channel is. An interesting FELIX-induced fragment peak is found at mass 79. The infrared spectrum encoded into this mass channel is displayed in Figure 7, and it is clearly different from that found on the benzoic acid fragment peaks. One obvious difference is the red shift of the CO stretching band of almost 200 cm^{-1}.

Assuming that protonation occurs at the most electronegative site of the benzoic acid molecule, being the carbonyl oxygen atom, the red shift of the CO stretching mode can be explained in terms of the removal of electron density from the C=O bond,
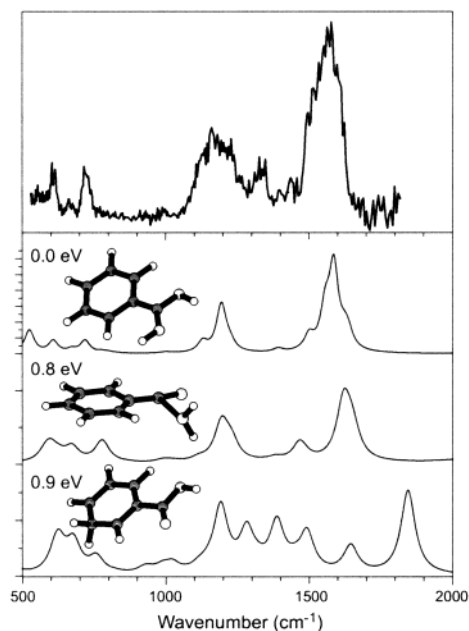
Figure 7. Infrared spectrum observed on fragment mass channel 79 (upper panel) compared to DFT calculated spectra (unscaled) of different possible structures of protonated benzoic acid. Relative structural energies at the B3LYP/D95(d,p) level of theory are indicated.

effectively reducing the bond order and hence the vibrational frequency. To verify this hypothesis, DFT calculations were run for protonation at the aromatic ring, the hydroxyl oxygen, and the carbonyl oxygen. The resulting structures, relative energies, and vibrational spectra are shown in Figure 7. The theory indicates that protonation at the hydroxyl oxygen leads to a structure with a very long hydroxyl C–O bond (2.70 Å), where elimination of a water molecule would only cost about 0.5 eV. Protonation of the aromatic ring occurs at one of the carbon atoms rather than on the π cloud.[27] The lowest energy structure is indeed found to be that where the proton attaches to the carbonyl oxygen atom. The infrared spectrum for this structure shows a remarkable agreement with the experimental spectrum. Only the band observed near 1330 cm^{-1} remains unaccounted for. The apparent broadening of the CO stretching band is caused by the strong coupling with the CC stretching modes between 1500 and 1600 cm^{-1}. Although the spectral match with the second structure appears to be reasonable in this wavelength range as well,[42] this structure can be excluded since infrared-induced dissociation would almost certainly lead to elimination of the water molecule and hence result in a fragment mass of 105 instead of 79. Hence, these results suggest that benzoic acid protonates at the carbonyl oxygen and that dissociation eliminates a carbon dioxide molecule, leaving behind the ion at mass 79, which likely corresponds to protonated benzene.

4. Conclusions

The infrared spectrum of the benzoic acid radical cation is recorded via IRMPD spectroscopy, which, to our knowledge, constitutes the first infrared spectrum of this species. Two different gentle ionization methods, REMPI and chemical ionization, are applied to produce the intact benzoic acid cation, which is mass selectively stored in a quadrupole ion trap. In general, REMPI schemes require knowledge of the electronic structure of the parent molecule as well as the availability of a pulsed tunable laser system. On the other hand, chemical ionization relies on the IP of the parent ion relative to that of the charge donor(s), which, in this study, are simply the ionic

UV-photofragments of benzoic acid. In addition, it is shown that this method can be used to study protonated species, obviously depending on the relative proton affinities of the target molecule and the proton donor(s).

The experimental spectrum indicates that the benzoic acid ion is effectively planar under our experimental conditions, whereas the B3LYP functional predicts a staggered geometry to be the lowest energy structure. This can be understood from the low barrier to planarity, which is much lower than the thermal energy available to the ion at room temperature, resulting in an essentially planar structure. The infrared spectrum of protonated benzoic acid, and in particular the large red shift of the CO stretch vibration, indicates that protonation takes place at the carbonyl oxygen.

References and Notes

(1) Duncan, M. A. *Int. J. Mass Spectrom.* **2000**, *200*, 545.

(2) Schwarz, H. A. *J. Chem. Phys.* **1977**, *67*, 5525.

(3) Oka, T. *Phys. Rev. Lett.* **1980**, *45*, 531.

(4) Gudeman, C. S.; Begemann, M. H.; Pfaff, J.; Saykally, R. J. *Phys. Rev. Lett.* **1983**, *50*, 727.

(5) Hilpert, G.; Linnartz, H.; Havenith, M.; ter Meulen, J. J.; Meerts, W. L. *Chem. Phys. Lett.* **1994**, *219*, 384. Anderson, D. T.; Davis, S.; Zwier, T. S.; Nesbitt, D. J. *Chem. Phys. Lett.* **1996**, *258*, 207. Park, J.; Xia, C.; Selby, S.; Foster, S. C. *J. Mol. Spectrosc.* **1996**, *179*, 150.

(6) Müller-Dethlefs, K.; Schlag, E. W. *Annu. Rev. Phys. Chem.* **1991**, *42*, 109.

(7) Zhu, L.; Johnson, P. *J. Chem. Phys.* **1991**, *94*, 5769.

(8) Okumura, M.; Yeh, L. I.; Myers, J. D.; Lee, Y. T. *J. Chem. Phys.* **1986**, *85*, 2328. Piest, H.; von Helden, G.; Meijer, G. *Astrophys. J.* **1999**, *520*, L75. Dopfer, O.; Olkhov, R. V.; Maier, J. P. *J. Chem. Phys.* **1999**, *111*, 10754. Fujii, A.; Fujimaki, E.; Ebata, T.; Mikami, N. *J. Chem. Phys.* **2000**, *112*, 6275.

(9) Taylor, D. P.; Goode, J. G.; LeClaire, J. E.; Johnson, P. M. *J. Chem. Phys.* **1995**, *103*, 6293. Fujii, A.; Iwasaki, A.; Ebata, T.; Mikami, N. *J. Phys. Chem. A* **1997**, *101*, 5963. Gerhards, M.; Schiwek, M.; Unterberg, C.; Kleinermanns, K. *Chem. Phys. Lett.* **1998**, *297*, 515.

(10) Grant, E. R.; Schulz, P. A.; Sudbo, A. S.; Shen, Y. R.; Lee, Y. T. *Phys. Rev. Lett.* **1978**, *40*, 115.

(11) Bagratashvili, V. N.; Letokhov, V. S.; Makarov, A. A.; Ryabov, E. A. *Multiple photon infrared laser photophysics and photochemistry*; Harwood: Chur, 1985.

(12) Shin, S. K.; Beauchamp, J. L. *J. Am. Chem. Soc.* **1990**, *112*, 2066. Peiris, D. M.; Cheeseman, M. A.; Ramanathan, R.; Eyler, J. R. *J. Phys. Chem.* **1993**, *97*, 7839. Stephenson, J. L.; Booth, M. M.; Shalosky, J. A.; Eyler, J. R.; Yost, R. A. *J. Am. Soc. Mass Spectrom.* **1994**, *5*, 886.

(13) Dunbar, R. C. *Int. J. Mass Spectrom.* **2000**, *200*, 571.

(14) Oomens, J.; van Roij, A. J. A.; Meijer, G.; von Helden, G. *Astrophys. J.* **2000**, *542*, 404.

(15) Asmis, K. R.; Brümmer, M.; Kaposta, C.; Santambrogio, G.; von Helden, G.; Meijer, G.; Rademann, K.; Wöste, L.; *Phys. Chem. Chem. Phys.* **2002**, *4*, 1101.

(16) Lemaire, J.; Boissel, P.; Heninger, M.; Mauclaire, G.; Bellec, G.; Mestdagh, H.; Simon, A.; Le Caer, S.; Ortega, J. M.; Glotin, F.; Maitre, P. *Phys. Rev. Lett.* **2002**, *89*, 273002.

(17) Moore, D. T.; Oomens, J.; van der Meer, L.; von Helden, G.; Meijer, G.; Valle, J.; Marshall, A. G.; Eyler, J. R. *Chem. Phys. Chem.* **2004**, *5*, 740.

(18) Oomens, J.; Meijer, G.; von Helden, G. *J. Phys. Chem. A* **2001**, *105*, 8302.

(19) Oomens, J.; Sartakov, B. G.; Tielens, A. G. G. M.; Meijer, G.; von Helden, G. *Astrophys. J.* **2001**, *560*, L99.

(20) Oomens, J.; Bakker, J. M.; Sartakov, B. G.; Meijer, G.; von Helden, G. *Chem. Phys. Lett.* **2003**, *367*, 576.

(21) van Heijnsbergen, D.; von Helden, G.; Meijer, G.; Maitre, P.; Duncan, M. A. *J. Am. Chem. Soc.* **2002**, *124*, 1562.

(22) Florio, G. M.; Sibert, E. L.; Zwier, T. S. *Faraday Discus.* **2001**, *118*, 315. Walther, M.; Plochocka, P.; Fischer, B.; Helm, H.; Jepsen, P. U. *Biopolymers* **2002**, *67*, 310.

(23) Nagaoka, S.; Hirota, N.; Matsushita, T.; Nishimoto, K. *Chem. Phys. Lett.* **1982**, *92*, 498. Stepanian, S. G.; Reva, I. D.; Radchenko, E. D.; Sheina, G. G. *Vibr. Spectrosc.* **1996**, *11*, 123. Remmers, K.; Meerts, W. L.; Ozier, I. *J. Chem. Phys.* **2000**, *112*, 10890.

(24) Bakker, J. M.; MacAleese, L.; von Helden, G.; Meijer, G. *J. Chem. Phys.* **2003**, *119*, 11180.

(25) Meijer, G.; de Vries, M. S.; Hunziker, H. E.; Wendt, H. R. *J. Phys. Chem.* **1990**, *94*, 4394.

(26) Solcà, N.; Dopfer, O. *Chem. Phys. Lett.* **2001**, *342*, 191.

(27) Solcà, N.; Dopfer, O. *Angew. Chem., Int. Ed. Engl.* **2002**, *41*, 3628.

(28) Jones, W.; Boissel, P.; Chiavarino, B.; Crestoni, M. E.; Fornarini, S.; Lemaire, J.; Maitre, P. *Angew. Chem., Int. Ed. Engl.* **2003**, *42*, 2057.

(29) Inokuchi, Y.; Nishi, N. *J. Phys. Chem. A* **2003**, *107*, 11319.

(30) Paul, W. *Rev. Mod. Phys.* **1990**, *62*, 531.

(31) March, R. E.; Todd, J. F. J. *Practical aspects of ion trap mass spectrometry, Volume I: Fundamentals of ion trap mass spectrometry*; CRC Press: Boca Raton, 1995.

(32) March, R. E. *J. Mass Spectrom.* **1997**, *32*, 351.

(33) Oepts, D.; van der Meer, A. F. G.; van Amersfoort, P. W. *Infrared Phys.* **1995**, *36*, 297. Or see the FELIX website: http://www.rijnh.nl/molecular-and-laser-physics/felix.

(34) Michael, S. M.; Chien, M.; Lubman, D. M. *Rev. Sci. Instrum.* **1992**, *63*, 4277.

(35) Oomens, J.; Tielens, A. G. G. M.; Sartakov, B. G.; von Helden, G.; Meijer, G. *Astrophys. J.* **2003**, *591*, 968.

(36) Oomens, J.; Moore, D. T.; Meijer, G.; von Helden, G. *Phys. Chem. Chem. Phys.* **2004**, *6*, 710.

(37) NIST Chemistry Webbook: http://webbook.nist.gov/chemistry/

(38) Frisch, M. J.; Trucks, G. W.; Schlegel, H. B.; Scuseria, G. E.; Robb, M. A.; Cheeseman, J. R.; Zakrzewski, V. G.; Montgomery, J. A., Jr.; Stratmann, R. E.; Burant, J. C.; Dapprich, S.; Millam, J. M.; Daniels, A. D.; Kudin, K. N.; Strain, M. C.; Farkas, O.; Tomasi, J.; Barone, V.; Cossi, M.; Cammi, R.; Mennucci, B.; Pomelli, C.; Adamo, C.; Clifford, S.; Ochterski, J.; Petersson, G. A.; Ayala, P. Y.; Cui, Q.; Morokuma, K.; Malick, D. K.; Rabuck, A. D.; Raghavachari, K.; Foresman, J. B.; Cioslowski, J.; Ortiz, J. V.; Stefanov, B. B.; Liu, G.; Liashenko, A.; Piskorz, P.; Komaromi, I.; Gomperts, R.; Martin, R. L.; Fox, D. J.; Keith, T.; Al-Laham, M. A.; Peng, C. Y.; Nanayakkara, A.; Gonzalez, C.; Challacombe, M.; Gill, P. M. W.; Johnson, B. G.; Chen, W.; Wong, M. W.; Andres, J. L.; Head-Gordon, M.; Replogle, E. S.; Pople, J. A. *Gaussian 98*, revision A.7; Gaussian, Inc.: Pittsburgh, PA, 1998.

(39) The neutral benzoic acid data have been convoluted with a 20-cm^{-1} full width at half maximum Lorentzian line shape for comparison with the IRMPD ion spectrum.

(40) Langhoff, S. R. *J. Phys. Chem.* **1996**, *100*, 2819.

(41) Pauzat, F.; Talbi, D.; Miller, M. D.; DeFrees, D. J.; Ellinger, Y. *J. Phys. Chem.* **1992**, *96*, 7882. Szczepanski, J.; Vala, M. *Astrophys. J.* **1993**, *414*, 646.

(42) Note that the bands around 1600 cm^{-1} in the calculated spectrum are due to CC stretching and HOH scissoring modes. The CO stretching band is calculated at 2275 cm^{-1}, outside the displayed range. See also ref 20.